Cyclohexene esterification–hydrogenation for green and efficient production of cyclohexanol

Zong Baoning[1], zhu yunfeng[1], gao liang[1], wen liangyou[1], Wang Hao[1], and Minghua Qiao[2]

[1]Affiliation not available
[2]Fudan University

July 7, 2020

Abstract

A novel process based on cyclohexene esterification–hydrogenation for the production of cyclohexanol, the key intermediate for the production of ε-caprolactam, was devised and validated for the first time. In this process, cyclohexene obtained from the partial hydrogenation of benzene is esterified with acetic acid to cyclohexyl acetate, followed by hydrogenation to cyclohexanol. The experimentally determined equilibrium conversion of cyclohexene for cyclohexene esterification at the stoichiometric ratio is always ?68% in the temperature range of 333–373 K over the commercial Amberlyst 15 catalyst, which is substantially higher than that of cyclohexene hydration. The apparent activation energy (Ea) for the esterification of cyclohexene with acetic acid is 60.0 kJ mol–1, also lower than that of cyclohexene hydration. On the other hand, the hydrogenation of cyclohexyl acetate to cyclohexanol is not thermodynamically limited, and high conversion of 99.5% and high selectivity of 99.7% are obtained on the La-promoted Cu/ZnO/SiO2 catalyst.

Technical heading: 5. Reaction Engineering, Kinetics and Catalysis

Keywords

Cyclohexanol, cyclohexene, acetic acid, esterification, hydrogenation

1. INTRODUCTION

ϵ -Caprolactam is the monomer of nylon-6 (polycaprolactam). The huge demand across the industries, such as packaging, electrical and electronics, consumer goods and appliances, and automotive greatly increase the overall ϵ -caprolactam consumption in the nylon-6 industry.[1,2] The estimated market value ofϵ -caprolactam is projected to reach $18.6 billion by 2019.[3] The industrial manufacture ofϵ -caprolactam involves a multiple-step transformation of benzene to cyclohexanone and/or cyclohexanol, with the latter can be facilely converted to the former by dehydrogenation, and the transformation of cyclohexanone to ϵ -caprolactam.[1] Cyclohexanol is also a key precursor of adipic acid, one of the monomers for nylon-66 (poly(hexamethylene adipamide)).[4] Thomas and Raja have skillfully developed a green one-step process to bridge the gap between cyclohexanone and ϵ -caprolactam by using redox and acid sites co-existing on the metal-doped nanoporous aluminophosphates (AlPOs) in tandem, thus avoiding the use of corrosive oleum and sulfuric acid and the generation of unwanted ammonium sulfate.[5]

However, the existing industrial processes for the production of cyclohexanone/cyclohexanol is far from safe, efficient, or atom-economic. Currently, there are three industrialized processes for this purpose, namely, (i) cyclohexane oxidation, (ii) cyclohexene hydration, and (iii) phenol hydrogenation (Scheme 1). The first process, though prevailing, is restricted by a low conversion of 4.5% to sustain a high selectivity of 93% (Table S1). In addition, the cyclohexane/air mixture is of high explosion risk, which has resulted in one of the most devastating accidents in the history of petrochemical industry.[6] The second process was developed

by Asahi Chemical in the late 1980s. Albeit cyclohexene hydration gives high cyclohexanol selectivity of 99.3%, the reaction is of low efficiency due to the poor miscibility of cyclohexene with water (200 ppm at 298 K[7] and 500 ppm at 393 K simulated by Aspen Plus). Moreover, the equilibrium conversion of cyclohexene hydration is only about 12.7%.[8,9] For the third process, while phenol hydrogenation to cyclohexanol can be highly selective,[10] the production of phenol is complicated, which involves the alkylation of benzene with propylene, cumene oxidation to cumene hydroperoxide, and cleavage of cumene hydroperoxide to phenol.[11] Furthermore, analogous to cyclohexane oxidation, cumene oxidation must be kept at a low conversion of 25% and is of high explosion risk.

Figure 1 illustrates the overall atom economy and per pass yield of cyclohexanol (including cyclohexanone for the first process) via these three processes starting from benzene based on the industrial and literature data compiled in Table S1. According to Trost, atom economy is defined as how much of the reactants end up in the product.[12] Herein, the reactant refers to benzene, and the product refers to cyclohexanol. The overall atom economy is in the order of 83.7% (Process 1) < 95.5% (Process 3) < 99.3% (Process 2). However, because of the bottlenecks either in selectivity (Processes 1 and 3) or in thermodynamics (Process 2), the per pass yield of cyclohexanone/cyclohexanol is low and is in the order of 3.7% (Process 1) < 5.1% (Process 2) < 14.9% (Process 3). In industry, the cyclohexanol yield is improved by massively circulating the unreacted feedstocks, which greatly adds up to the energy demand.

Aside from three industrial processes mentioned above, other processes, including cyclohexene esterification–transesterification and esterification–hydrolysis, have been widely investigated to produce cyclohexanol. However, for the former process, ether formation and olefin formation are common side reactions during transesterification.[13–15] Besides, like esterification reactions, transesterification reactions are typical, equilibrium limited reactions.[15,16] These drawbacks greatly increase the cost of product separation, thus inhibiting this process from practical application. For the latter process, the hydrolysis step in particular is very complex due to multiple reactions, phase splitting, and mismatch between the reaction conditions and separation conditions. Furthermore, the energy requirement is very high.[17,18] Hence, Freund and co-workers concluded that unless a right catalyst can be developed, this process is economically not viable.[19]

Herein, we report a novel cyclohexene esterification–hydrogenation process for the production of cyclohexanol (Scheme 2). In this process, cyclohexene obtained from the partial hydrogenation of benzene[20] is esterified with acetic acid to cyclohexyl acetate. The latter is then hydrogenated to cyclohexanol. We found that the experimentally determined equilibrium conversion for cyclohexene esterification at the stoichiometric ratio is always [?]68% in the temperature range of 333–373 K, which is substantially higher than that of cyclohexene hydration. And, the hydrogenation of ester to alcohol is not thermodynamically limited and is usually of high conversion and selectivity.[21] The additional merit is that the hydrogenation of cyclohexyl acetate simultaneously yields ethanol that is widely used as antiseptic, solvent, and fuel or fuel additive. Therefore, the novel cyclohexene esterification–hydrogenation process devoid of the shortcomings of the existing industrial processes is highly promising to produce cyclohexanol in a safe, efficient, and green manner.

2. EXPERIMENTAL

2.1 Chemicals

If not specified, the chemicals were of analytic grade. Benzene, cyclohexene (A.R.), acetic acid (A.R.), $Cu(NO_3)_2$[?]$3H_2O$, $Zn(NO_3)_2$[?]$6H_2O$, $Na_2SiO_3 \cdot 9H_2O$, and NaOH were purchased from Sinopharm Chemical Reagent. Amberlyst 15 and $La(NO_3)_3$[?]$6H_2O$ were purchased from J&K. The gases were purchased from Beijing Haipu Gas.

2.2 Esterification of cyclohexene with acetic acid

2.2.1 Thermodynamic study

Thermodynamic studies were carried out on METLER TOLEDO RC1 reaction calorimeter fitted with an MP06 medium-pressure 500 mL-capacity glass autoclave. Prior to the reaction, 100 g of Amberlyst 15 were

dried at 378 K for 24 h until the content of water in the catalyst was below 1% as determined by the Karl Fischer method. The autoclave containing the catalyst was sealed and pressurized to 0.6 MPa with $N_2$for air tightness test. Then, the autoclave was pressurized to 0.3 MPa, and cyclohexene and acetic acid with a total weight of 200 g were pumped into the autoclave with a prescribed acetic acid/cyclohexene ratio. After being heated to the desired temperature for a certain period, the liquid was sampled and analyzed gas chromatographically. The attainment of the equilibrium of esterification was judged based on the detection that the compositions of the liquid in two successive analyses were identical.

2.2.2 Kinetic study

The kinetic studies were conducted on a plug-flow fixed-bed reactor. The experimental set-up is depicted in Figure S1. The tubular reactor with the inner diameter of 4 mm and length of 10 cm was made of 316L stainless steel. Amberlyst 15 was dried at 378 K for 24 h until the content of water in the catalyst was below 1% as determined by the Karl Fischer method. Then, 1.0 g of the catalyst ($d_{\mathrm{p}} < 0.5$ mm) diluted with quartz sand (0.1 mm $< d_{\mathrm{p}} < 0.8$ mm) to avoid temperature runaway was loaded in the reaction zone. The remaining space was filled with quartz sand. Prior to the reaction, the catalyst bed was further purged with N_2 at 373 K to remove water. After being cooled down to below the reaction temperature, cyclohexene and acetic acid with a prescribed molar ratio was continuously pumped into the reactor at a flow rate 60 g h^{-1}. Each study was last for 2–3 h, during which the effluent was sampled several times to ensure that the reaction has reached the steady state. The reaction rate is calculated as follows:

in which C6 represents cyclohexene, while C6E represents the resulting ester. x represents the molar fraction, which is dimensionless.F is the total molar flow rate in mol h^{-1}. And$W$ represents the catalyst mass with unit in kg. Both the thermodynamic and kinetic studies were repeated at least twice.

2.3 Hydrogenation of cyclohexyl acetate

2.3.1 Catalyst preparation

The Cu/ZnO-based hydrogenation catalysts were prepared by the co-precipitation method. In a typical synthesis, 1 mol of copper nitrate, 1 mol of zinc nitrate, and 2 mol of sodium silicate were respectively dissolved in 500 mL of deionized water. The solutions were simultaneously added dropwise into a beaker in 1 h at room temperature under mechanical stirring at 500 rpm. The precipitates were formed during the addition. Then, the precipitates were aged for 12 h. The precipitates were filtrated and washed 10 times with deionized water. The filter cake was dried at 383 K for 24 h and calcined at 623 K with a heating rate of 5 K min^{-1} for 12 h. The resulting catalyst precursor was pelletized, crushed, sieved to 30–50 meshes, and denoted as $Cu_1Zn_1Si_2$.

The Cu_x Zn_1Si_2catalysts (x = 0, 0.5, 0.75, 1, 1.25, 1.5, and 2) and Cu_y Zn_{2-y} Si_2catalysts (y = 0.5, 0.75, 1, 1.25, 1.5, 1.75, and 2) were prepared by the procedures described above except for the amounts of the copper and zinc salts used. The $Cu_1Zn_1Si_2La_{0.1}$catalyst was also prepared in a similar manner except for the addition of 0.1 mol of lanthanum nitrate during the preparation.

2.3.2 Catalytic testing

The activity test was conducted on a continuous flow high-pressure unit equipped with a stainless-steel fixed-bed tubular reactor with a length of 1.2 m and an inner diameter of 1 cm with a height of approximately 15 cm. In a typical testing, 10 g of the as-prepared catalyst diluted with quartz sand of the same size to 12 mL was loaded in the reactor. Both sides of the catalyst bed were packed with quartz sand. The catalyst was activated in H_2 flow (200 mL $min^{-1}$and 3 MPa) at 493 K for 24 h at a ramping rate of 10 K min^{-1}. After being cooled down to the reaction temperature of 483 K, cyclohexyl acetate was pumped into the reactor at 5.0 g h^{-1} with the H_2/ester molar ratio of 30 and a system pressure of 5 MPa. The reaction reached the steady state after 12 h on stream. Then, the product was sampled every 12 h for at least three times, and each sample was analyzed three times gas chromatographically. The catalysts were evaluated at least in duplicate.

2.4 Product analysis

The esterification and hydrogenation products were analyzed on an Agilent 7890A gas chromatograph equipped with a flame ionization detector (FID) and an HP PONA capillary column (50 m x 0.2 mm x 0.5 μm). During the analysis, the flow rate of the N_2 carrier gas was 0.2 mL min^{-1}. The flow rates of H_2 and air were 30 mL min^{-1} and 400 mL min^{-1}, respectively. The temperatures of the injector and FID were both 523 K. The initial temperature of the column was set at 333 K, which was raised to 473 K at the heating rate of 5 K min^{-1} and maintained for 15 min. The column temperature was further raised to 513 K at a heating rate of 5 K min^{-1} and maintained for 50 min.

On the basis of the chromatographic results, the conversion of cyclohexene during esterification was calculated as (initial moles of cyclohexene – moles of cyclohexene after reaction)/(initial moles of cyclohexene) × 100%. The selectivity to cyclohexyl acetate was calculated as (moles of cyclohexyl acetate after reaction)/(initial moles of cyclohexene) × 100%.

The conversion of cyclohexyl acetate during hydrogenation was calculated as (initial moles of cyclohexyl acetate – moles of cyclohexyl acetate after reaction)/(initial moles of cyclohexyl acetate) × 100%. The selectivity to cyclohexanol was calculated as (moles of cyclohexanol after reaction)/(initial moles of cyclohexyl acetate) × 100%.

2.5 Characterization techniques

N_2 physisorption was conducted at 77 K on a Micromeritics Tristar 3000 apparatus. Prior to the measurements, the acid resin catalyst was outgassed at 343 K for 8 h. The bulk composition of the catalyst was determined by the inductively coupled plasma-atomic emission spectroscopy (ICP–AES; Thermo Elemental IRIS Intrepid). Exactly 200 mg of the catalyst was added to 20 mL of 25 wt% HNO_3 solution and heated to boiling. Then, 20 mL of 40% of HF was added and stirred vigorously. The solution was diluted to 200 mL with distilled water for analysis. The XRD pattern was acquired on a Philips X'Pert Pro powder X-ray diffractometer using Cu Kα radiation ($\lambda = 0.15418$ nm). The tube voltage was 40 kV, and the current was 40 mA. The 2θ angles were scanned from 10 to 70° at 10° min^{-1}. TEM characterization and elemental mapping were conducted on an FEI TECNAI F20 G2 electron microscope operated at 200 kV, to which a Gatan GIF 2001 spectrometer was attached. The energy filter images were recorded under the EFTEM mode. The width of the energy filter slit was 10 eV, the GIF incidence aperture was 0.6 mm, and the 3-window method was applied during elemental mapping collection.

3. RESULTS AND DISCUSSION

3.1 Esterification of cyclohexene with acetic acid

Since the thermodynamic parameters of the reaction of esterification of cyclohexene with acetic acid to cyclohexyl acetate has not been tackled before,[13] and the thermodynamic properties of cyclohexyl acetate are lacking, we experimentally determined the equilibrium conversion of cyclohexene at different acetic acid/cyclohexene molar ratios and temperatures using Amberlyst 15 as the catalyst. Many solid acid catalysts, such as silica-supported HPA (HSiW) or $H_3PW_{12}O_{40}$, sulfated zirconia, and ion-exchange resins, have been used for the esterification of olefins with acids.[22-24] Amberlyst 15 is a commercially available, strongly acidic macroreticular polymeric resin based on crosslinked styrene, which is one of the most frequently used ion-exchange resins in acid-catalyzed reactions.[22] In particular, Saha and Sharma reported that Amberlyst 15 was more active than the Amberlite IR-120 genular resin, Engelhard F-24 acid-treated clay, and homogeneous *p* -toluene sulphonic acid catalysts in cyclohexene esterification with formic acid.[25]Chakrabarti and Sharma found that Amberlyst 15 was more active than Engelhard F-24 in cyclohexene esterification with acetic acid.[13] As plotted in Figure 2a, the equilibrium conversion of cyclohexene decreases with the increase in the temperature, reflecting that the esterification of cyclohexene with acetic acid is exothermic. The cyclohexene conversion is improved when increasing the acetic acid/cyclohexene ratio as expected. At the stoichiometric acetic acid/cyclohexene ratio of 1, the cyclohexene conversion is 79.1% at 333 K, which decreases gradually to 68.0% at 373 K. When the acetic acid/cyclohexene ratio is elevated to 3, the cy-

clohexene conversion amounts to 93.5% at 333 K, which decreases to 85.1% at 373 K. Nevertheless, the cyclohexene conversion at the stoichiometric ratio at 373 K is still much higher than the conversion of 12.7% via the route of cyclohexene hydration.[8] In addition, the selectivity to cyclohexyl acetate remains as high as 99.7% at 343 K, which decreases slightly to <98% at 363 K and above owing to the occurrence of the oligomerization/isomerization of cyclohexene in the presence of the acid catalyst. These by-products have also been identified in cyclohexene hydration.[7]

Assuming that the enthalpy change (ΔH °) and entropy change (ΔS °) are constant in the temperature range investigated, the relationship between the reaction equilibrium constant (K) and the reaction temperature can be expressed as:

On the basis of the data in Figure 2A, we obtained a good linear relationship between $\ln K$ and $1/T$ (Figure 2B). From the intercept and slope of the line, the following thermodynamic parameters for the esterification of cyclohexene with acetic acid to cyclohexyl acetate are derived: ΔH ° = –22860.8 ± 2825.4 J mol^{-1}, ΔS ° = –42.8 ± 8.0 J mol^{-1} K^{-1}, and ΔG ° = –22860.8 + 42.8T J mol^{-1} in the temperature range of 333–373 K. It should be noted that the ΔG ° for this reaction is far more negative than that for cyclohexene hydration (365 J mol^{-1} at 333 K and 7339 J mol^{-1} at 373 K, calculated by HSC5.0 software), unambiguously confirming that esterification of cyclohexene with acetic acid is thermodynamically more favorable than cyclohexene hydration.

Figure 3 shows the reaction rates of cyclohexene esterification at various acetic acid/cyclohexene ratios and reaction temperatures on a fixed-bed reactor (Figure S1). The effects of external and internal diffusion have been eliminated (Figure S2). The reaction temperature drastically affects the esterification rate of cyclohexene, which in general doubles with a 10 K-increment in the reaction temperature. Besides, the reaction rate decreases with the increase in the acetic acid/cyclohexene ratio. It is plausible that cyclohexene adsorbs much weaker than acetic acid on Amberlyst 15, considering that acetic acid can interact tightly with the sulfonic acid groups on Amberlyst 15 via hydrogen bonding. Hence, the adsorption of cyclohexene is the key factor that limits the reaction. The weak adsorption of cyclohexene with respect to acetic acid on the same active sites is substantiated by the fitting results of the reaction data in Figure 3 using the Langmuir–Hinshelwood–Hougen–Watson (LHHW) type kinetics model. As compiled in Table S2, the reaction parameters derived from the LHHW-type kinetics model show that the adsorption equilibrium constant of cyclohexene is much smaller than that of acetic acid. Moreover, the apparent activation energy (E_a) of the esterification of cyclohexene with acetic acid is 60.0 kJ mol^{-1}, which is lower than theE_a of 71.2 kJ mol^{-1} for cyclohexene hydration.[26] Therefore, these experimental results substantiate that the esterification of cyclohexene with acetic acid is both thermodynamically and kinetically more advantageous than cyclohexene hydration.

3.2 Hydrogenation of cyclohexyl acetate to cyclohexanol

Since the hydrogenation of cyclohexyl acetate to cyclohexanol has also not been explored to the best of our knowledge, we developed the Cu/ZnO/SiO_2 catalysts for this purpose. The number of catalyst systems allowing the production of alcohols from ester hydrogenation is limited. The catalysts of choice, which allow the highly selective conversion of esters to alcohols, are mostly based on Cu.[27–29] Besides, the Cu-based catalysts are more cost-effective than the noble metal-based catalysts for this purpose,[30] which is an important factor to be considered for a reaction with significant industrial background. ZnO is capable of dispersing and stabilizing Cu nanoparticles to replace the conventional copper chromite catalysts that are hazardous to the environment.[27,31] SiO_2 was adopted as the support, since it is not only able to disperse Cu,[27] but also weakly acidic in nature and would not lead to considerable undesired intramolecular/intermolecular dehydration or isomerization of the hydrogenation products.

Firstly, we systematically examined the effects of the contents of Cu and the Cu/Zn molar ratios on the catalytic performances of the Cu/ZnO/SiO_2 catalysts in the hydrogenation of cyclohexyl acetate. As summarized in Table S3, over the $Cu_0Zn_1Si_2$ catalyst without Cu, the hydrogenation reaction did not occur. When increasing the contents of Cu while fixing the Zn: Si molar ratio at 1: 2, the conversion of cyclohexyl acetate increased drastically, reaching a maximum over the $Cu_1Zn_1Si_2$ catalyst, manifesting that Cu is the active

center for ester hydrogenation. When further increasing the contents of Cu, the conversion of cyclohexyl acetate declined monotonically, which is attributed to the agglomeration of excessive Cu. A similar effect of the content of Cu on the hydrogenation activity was observed on the $Cu/ZnO/Al_2O_3$ catalysts for the hydrogenation of ethyl acetate.[32] When altering the Cu/Zn molar ratio while fixing the (Cu + Zn): Si molar ratio at 2: 2, the conversion of cyclohexyl acetate evolved in a volcanic shape. At low Cu/Zn ratio, there was no sufficient active centers for ester hydrogenation, while at high Cu/Zn ratio, there was no sufficient ZnO to disperse Cu, thus an optimal Cu/Zn molar ratio occurred at 1: 1. An optimal Cu/Zn ratio was also identified for the CuZn–SiO_2 bimetallic catalysts in the hydrogenation of methyl acetate.[33] Among the $Cu/ZnO/SiO_2$ catalysts investigated, the $Cu_1Zn_1Si_2$ catalyst displayed the highest conversion of 99.5% and the highest cyclohexanol selectivity of 98.3% under identical reaction conditions of 483 K, 5.0 MPa, H_2/ester molar ratio of 30, and weight hourly space velocity (WHSV) of 0.5 h^{-1}. As anticipated, there were only trace amounts of the acid-catalyzed by-products including ethyl acetate, cyclohexane, and cyclohexyl ether.

To further improve the selectivity, we in situ modified the $Cu_1Zn_1Si_2$ catalyst during the co-precipitation process by adding 0.1 molar fraction of La relative to Cu (denoted as $Cu_1Zn_1Si_2La_{0.1}$). The modification effects of lanthanum oxide have been reported to be originated from several aspects, such as the textural change in catalyst to form basic active sites and the improvement of the surface area of the catalyst.[34,35] The basic physicochemical properties of the $Cu_1Zn_1Si_2La_{0.1}$and $Cu_1Zn_1Si_2$ catalysts are presented in Table S4. As anticipated, the basicity of lanthanum oxide further suppressed the occurrence of the acid-catalyzed reactions during the hydrogenation of cyclohexyl acetate, which improved the cyclohexanol selectivity up to 99.7%, while did not impose an adverse effect on the conversion (Table S3 and Figure 4). Moreover, increasing the WHSV from 0.5 to 1.1 h^{-1} did not change significantly the conversion and selectivity over the $Cu_1Zn_1Si_2La_{0.1}$catalyst (Table S3).

According to Table S4, the specific surface area (S_{BET}) of the $Cu_1Zn_1Si_2La_{0.1}$catalyst is larger than that of the $Cu_1Zn_1Si_2$ catalyst. The XRD patterns of the $Cu_1Zn_1Si_2$ and $Cu_1Zn_1Si_2La_{0.1}$catalysts in Figure 5A show that aside from the broad peak at $2\theta$of ˜25° from amorphous SiO_2, only the diffraction peaks due to metallic Cu (*fcc* Cu, JCPDS 04-0836) were identified, indicating that ZnO is in the amorphous state on both catalysts. The phase relating to La on the $Cu_1Zn_1Si_2La_{0.1}$catalyst was also not discerned, which is attributed to its low loading and/or high dispersion. The crystallite sizes of Cu calculated by the Scherrer formula in terms of X-ray line broadening are 18.0 nm and 14.8 nm for the $Cu_1Zn_1Si_2$ and $Cu_1Zn_1Si_2La_{0.1}$catalysts, respectively, which may account for the high conversion of cyclohexyl acetate when increasing the WHSV on the $Cu_1Zn_1Si_2La_{0.1}$catalyst. The HRTEM image of the $Cu_1Zn_1Si_2La_{0.1}$catalyst in Figure 5B shows only the Cu(111) lattice fringes with the interplanar spacing of 2.08 Å, while the lattice fringes of ZnO were not identified, which is consistent with the XRD result. The TEM image and particle size distribution histogram of the $Cu_1Zn_1Si_2La_{0.1}$catalyst in Figure 5C shows that the average particle size of Cu is 15.8 nm, which agrees well with the crystallite size derived from XRD.

Figures 5D–5I present the scanning transmission electron microscopic-energy dispersive spectroscopic (STEM–EDS) images of the $Cu_1Zn_1Si_2La_{0.1}$catalyst. Figure 5D is the HAADF–STEM image, Figures 5E–5H are the corresponding EDS mappings of Si, Cu, Zn, and La, and Figure 5I is the overlapping of Figures 5E–5H. Comparison of Figure 5D with Figure 5F readily leads to the conclusion that the bright particles in Figure 5D are originated from Cu. Comparison of Figure 5G with Figures 5D and 5F reveals that Zn is located preferentially on or in vicinity to Cu rather than distributed randomly on SiO_2, signifying that ZnO interacts strongly with Cu. This conclusion is additionally substantiated by Figure 5I. On the other hand, the distribution of La is homogeneous and does not show such a preference as that of Zn.

From the experimental results demonstrated above, we figured out the overall atom economy of 99.4% and the yield of cyclohexanol per pass of 34.6% for the novel cyclohexene esterification–hydrogenation process, as also demonstrated in Figure 1. The former is comparable to that of the most selective cyclohexene hydration process, whereas the latter is more than twice of that of the most efficient phenol hydrogenation process. It is evident that the cyclohexene esterification–hydrogenation process is highly advantageous in producing cyclohexanol in a safe, efficient, and green manner.

3.3 Pilot-scale cyclohexene esterification–hydrogenation

Taking into account of the reaction characteristics of cyclohexene esterification, we transferred this reaction onto a reactive distillation reactor, which is capable of breaking through the thermodynamic limitation imposed on the conversion while retaining the high reaction rate for the exothermic reaction.[36] On conventional slurry-phase reactor or fixed-bed reactor, the intrinsic conflict between the conversion and reaction rate in cyclohexene esterification cannot be disentangled. On the basis of the above experimental thermodynamic and kinetic data and Aspen Plus simulations, a reactive distillation reactor was built for cyclohexene esterification, on which the operation parameters were further experimentally optimized, which are out of the scope of the present work. The optimized operation parameters for the reactive distillation reactor are presented in Table S5. And the corresponding temperature and composition profiles in the reactive distillation reactor are illustrated in Figure S3. Then, we established a pilot-scale demonstration unit with a capacity of 8000 t/a using the reactive distillation reactor for cyclohexene esterification in conjugation with a fixed-bed reactor for ester hydrogenation at Baling Petrochemical Company, SINOPEC (Figure S4). On the reactive distillation reactor, the cyclohexene conversion is further improved to >99.2% with high selectivity to cyclohexyl acetate of ˜99.0% (Figure 6A). Moreover, the reaction proceeds smoothly for more than 1000 h on stream with no indication of deactivation.

The cyclohexyl acetate produced from the reactive distillation reactor was directly fed into the successive fixed-bed reactor for hydrogenation. Figure 6B shows that the conversion of cyclohexyl acetate is always close to 100%, and the cyclohexanol selectivity is always >99% during more than 1000 h on stream, giving rise to the conversion of 99.8% and the selectivity of 99.4% on average. In addition, the ethanol selectivity is 99.5% on average during the whole reaction span.

4. CONCLUSIONS

We successfully demonstrated the feasibility of the novel cyclohexene esterification–hydrogenolysis process for the production of cyclohexanol, the intermediate for the production ofϵ -caprolactam. The bench-scale studies verified that cyclohexene esterification is thermodynamically and kinetically more favorable than cyclohexene hydration. And the $Cu_1Zn_1Si_2La_{0.1}$catalyst afforded high conversion and selectivity in the hydrogenation of cyclohexyl acetate to cyclohexanol. The cyclohexene esterification–hydrogenation process was operated smoothly in a long term on a pilot-scale demonstration unit. Moreover, this process not only shows high overall atom economy comparable to the cyclohexene hydration process, but also exhibits much higher catalytic efficiency than the phenol hydrogenation process. This work elegantly bridges the gap between the Asahi's process of benzene partial hydrogenation to cyclohexene and Thomas and Raja's process of one-step transformation of cyclohexanone to ϵ -caprolactam, thus completing the last technological puzzle for the development of a next-generation process for the manufacture of nylon-6 from benzene in a safe, efficient, and green manner.

ACKNOWLEDGMENTS

This work was supported by the National Basic Research Program of China (2012CB224800), the Natural Science Foundation of China (20872035), and Technology Development Program of SINOPEC, China (S411063).

Literature cited

1. Weissermel K, Arpe HJ. Industrial Organic Chemistry, 4th ed., Wiley-VCH, Weinheim, 2003. 2. Mokaya R, Poliakoff M. A cleaner way to nylon? *Nature.*2005;437:1243-1244. 3. https://www.marketsandmarkets.com/PressReleases/caprolactam.asp. 4. Vafaeezadeh M, Hashemi MM. Dual catalytic function of the task-specific ionic liquid: Green oxidation of cyclohexene to adipic acid using

30% H_2O_2.*Chem Eng J.*2013;221:254-257. 5. Thomas JM, Raja R. Design of a "green" one-step catalytic production of ϵ-caprolactam (precursor of nylon-6). *Proc Natl Acad. Sci.* 2005;102(39):13732-13736. 6. Høiset S, Hjertager BH, Solberg T, Malo KA. Flixborough revisited - an explosion simulation approach. *J Hazardous Mater.*2000;77(1-3):1-9. 7. Zhang H, Mahajani SM, Sharma MM, Sridhar T. Hydration of cyclohexene with solid acid catalysts. *Chem Eng Sci.* 2002;57(3):315-322. 8. Ishida H. Liquid-phase hydration process of cyclohexene with zeolites. *Catal Surv Jpn.* 1997;1:241-246. 9. Meng FJ, Wang YQ, Wang SG, Wang SH. Hydration of cyclohexene over zeolite ZSM-5: Improved catalyst performance by alkali treatment.*React Kinet Mech Catal.* 2016;119(2):671-683. 10. Liu HZ, Jiang T, Han BX, Liang SG, Zhou YX. Selective phenol hydrogenation to cyclohexanone over a dual supported Pd–Lewis acid catalyst. *Science.* 2009;326(5957):1250-1252.

11. Schmidt RJ. Industrial catalytic processes - phenol production. *Appl Catal A.*2005;280(1):89-103.

12. Trost BM. The atom economy?A search for synthetic efficiency.*Science.* 1991; 254(5037):1471-1477.

13. Chakrabarti A, Sharma MM. Cyclohexanol from cyclohexene via cyclohexyl acetate: catalysis by ion-exchange resin and acid-treated clay. *React Polym.* 1992;18(2): 107-115.

14. Saha B, Streat M. Transesterification of cyclohexyl acrylate with$n$ -butanol and 2-ethylhexanol: acid-treated clay, ion exchange resins and tetrabutyl titanate as catalysts. *React Funct Polym.*1999;40(1):13–27.

15 Schmitt M, Hasse H. Chemical equilibrium and reaction kinetics of heterogeneously catalyzed n -hexyl acetate esterification.*Ind Eng Chem Res.* 2006;45(12):4123-4132.

16. Bożek-Winkler E, Gmehling J. Transesterification of methyl acetate and n -butanol catalyzed by Amberlyst 15. *Ind Eng Chem Res.*2006;45(20):6648-6654.

17. Steyer F, Sundmacher K. Cyclohexanol production via esterification of cyclohexene with formic acid and subsequent hydration of the esters?Reaction kinetics. *Ind Eng Chem Res.* 2007;46(4):1099-1104.

18. Kumar R, Katariya A, Freund H, Sundmacher K. Development of a novel catalytic distillation process for cyclohexanol production: Mini plant experiments and complementary process simulations. *Org Process Res Dev.* 2011;15(3):527-539.

19. Imam RA, Freund H, Guit RPM, Fellay C, Meier RJ, Sundmacher K. Evaluation of different process concepts for the indirect hydration of cyclohexene to cyclohexanol. *Org Process Res Dev.*2013;17(3):343-358.

20. Zhou GB, Dou RF, Bi HZ, Xie SH, Pei Y, Fan KN, Qiao MH, Sun B, Zong BN. Ru nanoparticles on rutile/anatase junction of P25 TiO_2: Controlled deposition and synergy in partial hydrogenation of benzene to cyclohexene. *J Catal.*2015;332:119-126.

21. Elangovan S, Garbe M, Jiao HJ, Spannenberg A, Junge K, Beller M. Hydrogenation of esters to alcohols catalyzed by defined manganese pincer complexes.*Angew Chem Int Ed.* 2016;55(49):15364-15368.

22. Hattori H, Ono Y. Solid Acid Catalysis, CRC Press, Boca Raton, 2015.

23. Gee JC, Fisher S. Direct esterification of olefins: The challenge of mechanism determination in heterogeneous catalysis. *J Catal.*2015;331:13-24.

24. Steyer F, Sundmacher K. VLE and LLE data set for the system cyclohexane + cyclohexene + water + cyclohexanol + formic acid + formic acid cyclohexyl ester. *J Chem Eng Data.* 2005;50(4):1277-1282.

25. Saha B, Sharma MM. Esterification of formic acid, acrylic acid and methacrylic acid with cyclohexene in batch and distillation column reactors: ion-exchange resins as catalysts. *React Funct Polym.*1996;28(3):263-278.

26. Ye JC, Huang JL, Lin HD, Cao KT, Sha Y. Kinetic-thermodynamic analysis of the reactive distillation process of the cyclohexene hydration using the aeolite catalyst. *Chin J Chem Eng.*2011;19(5):808-814.

27. Turek T, Trimm DL, Cant NW. The catalytic hydrogenolysis of esters to alcohols. *Catal Rev-Sci Eng.* 1994;36(4):645-683.

28. Chen LF, Guo PJ, Qiao MH, Yan SR, Li HX, Shen W, Xu HL, Fan KN. Cu/SiO_2 catalysts prepared by the ammonia-evaporation method: Texture, structure, and catalytic performance in hydrogenation of dimethyl oxalate to ethylene glycol. *J Catal.*2008;257:172-180.

29. Gong JL, Yue HR, Zhao YJ, Zhao S, Zhao L, Lv J, Wang SP, Ma XB. Synthesis of ethanol via syngas on Cu/SiO_2 catalysts with balanced Cu^0-Cu^+ sites. *J Am Chem Soc.* 2012;134(34):13922-13925.

30. Samal AK, Zhu HB, Harb M, Sangaru SS, Anjum DH, Hedhili MN, Saih Y, Basset JM. A general approach for the synthesis of bimetallic M–Sn (M = Ru, Rh and Ir) catalysts for efficient hydrogenolysis of ester.*Catal Sci Technol.* 2017;7(3):581-586.

31. Grunwaldt JD, Molenbroek AM, Topsøe NY, Topsøe H, Clausen BS. In situ investigations of structural changes in Cu/ZnO catalysts. *J Catal.* 2000;194(2):452-460.

32. Zhu YM, Shi L. Zn promoted Cu–Al catalyst for hydrogenation of ethyl acetate to alcohol. *J Ind Eng Chem.* 2014;20(4):2341-2347.

33. Zhao YJ, Shan B, Wang Y, Zhou JH, Wang SP, Ma XB. An effective CuZn–SiO_2 bimetallic catalyst prepared by hydrolysis precipitation method for the hydrogenation of methyl acetate to ethanol.*Ind Eng Chem Res.* 2018;57(13):526-4534.

34. Zheng XL, Lin HQ, Zheng JW, Duan XP, Yuan YZ. Lanthanum oxide-modified Cu/SiO_2 as a high-performance catalyst for chemoselective hydrogenation of dimethyl oxalate to ethylene glycol. *ACS Catal.* 2013;3(12):2738-2749.

35. Mo LY, Leong KKM, Kawi S. A highly dispersed and anti-coking Ni-La_2O_3/SiO_2 catalyst for syngas production from dry carbon dioxide reforming of methane.*Catal Sci Technol.* 2014;4(7):2107-2114.

36. Taylor R, Krishna R. Modelling reactive distillation. *Chem Eng Sci.* 2000;55(22):5183-5229.

FIGURE CAPTIONS

FIGURE 1 Comparison of the overall atom economy and per pass yield of cyclohexanol/cyclohexanone of the current industrial processes and the novel cyclohexene esterification–hydrogenation process from benzene.

FIGURE 2 (A) Effects of reaction temperature and acetic acid/cyclohexene molar ratio on cyclohexene conversion in cyclohexene esterification, and (B) a plot of $\ln K$ against $1/T$.

FIGURE 3 Influence of the acetic acid/cyclohexene molar ratio on the esterification rate of cyclohexene at various reaction temperatures. The curves are simulated by the LHHW-type kinetics model.

FIGURE 4 The chromatogram of the hydrogenation products of cyclohexyl acetate over the $Cu_1Zn_1Si_2La_{0.1}$catalyst.

FIGURE 5 (A) The XRD patterns of the $Cu_1Zn_1Si_2$ and $Cu_1Zn_1Si_2La_{0.1}$catalysts, (B) the HRTEM image, (C) the TEM image and particle size distribution histogram, (D) the HAADF–STEM image and the corresponding EDS mappings of (E) Si, (F) Cu, (G) Zn, (H) La, and (I) the overlapping of these elements of the $Cu_1Zn_1Si_2La_{0.1}$catalyst.

FIGURE 6 (A) The long-term evolutions of the conversion of cyclohexene and the selectivity to cyclohexyl acetate in the esterification of cyclohexene with acetic acid on the pilot-scale reactive distillation reactor. Reaction conditions: reboiler duty of 1050 W, total reflux at ambient pressure, acetic acid feed at the top of the column at 2.59 kg h^{-1}, cyclohexene feed at the middle of the catalytic section at 3.54 kg h^{-1}, and total catalyst loading of 2.65 kg, and (B) the long-term evolutions of the conversion of cyclohexyl acetate and the selectivities to cyclohexanol and ethanol in the hydrogenation of cyclohexyl acetate on the pilot-scale

fixed-bed reactor. Reaction conditions: temperature of 473 K, pressure of 6.2 MPa, H_2 flow rate of 100 L min^{-1}, cyclohexyl acetate feed rate of 870 g h^{-1}, and catalyst loading of 1.0 kg.

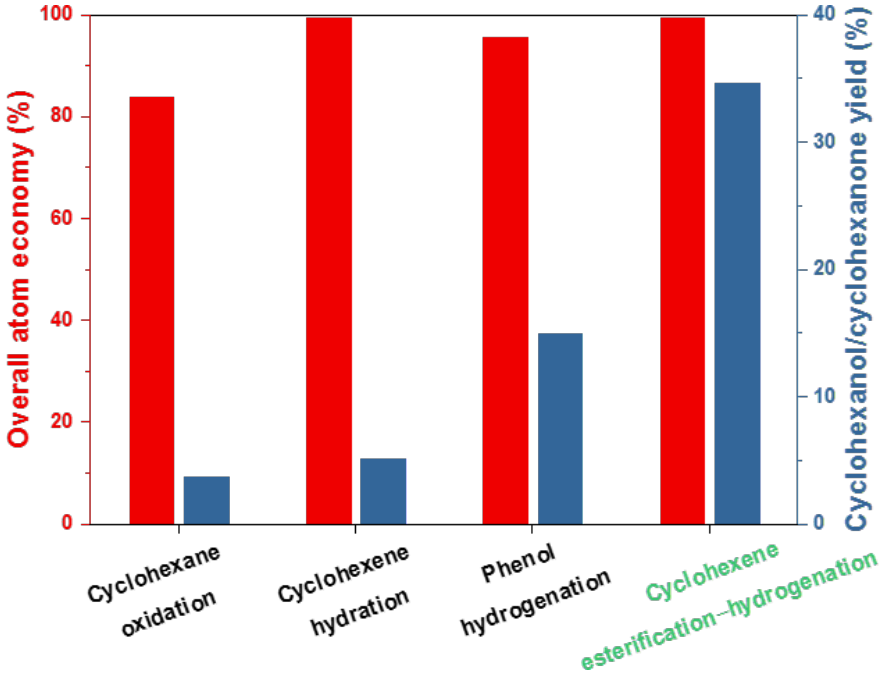

FIGURE 1

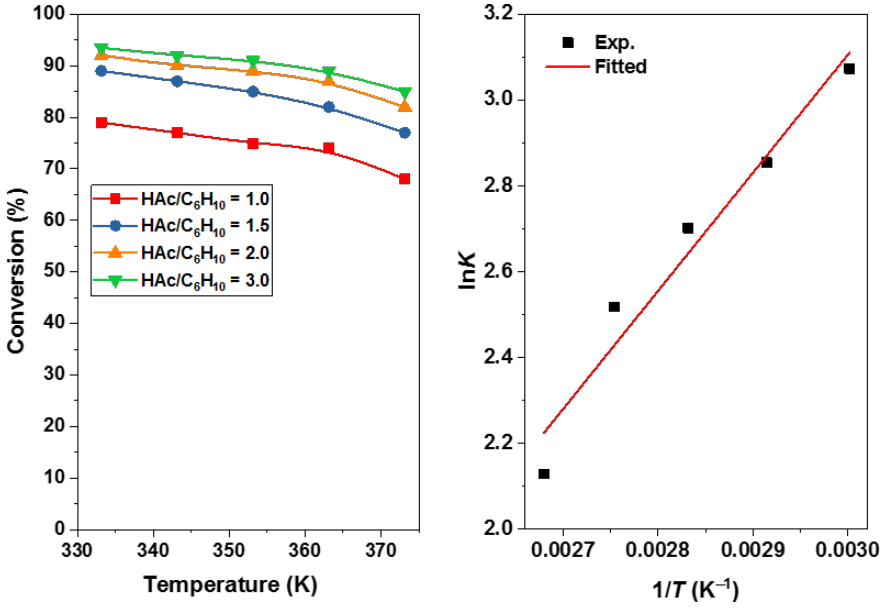

FIGURE 2

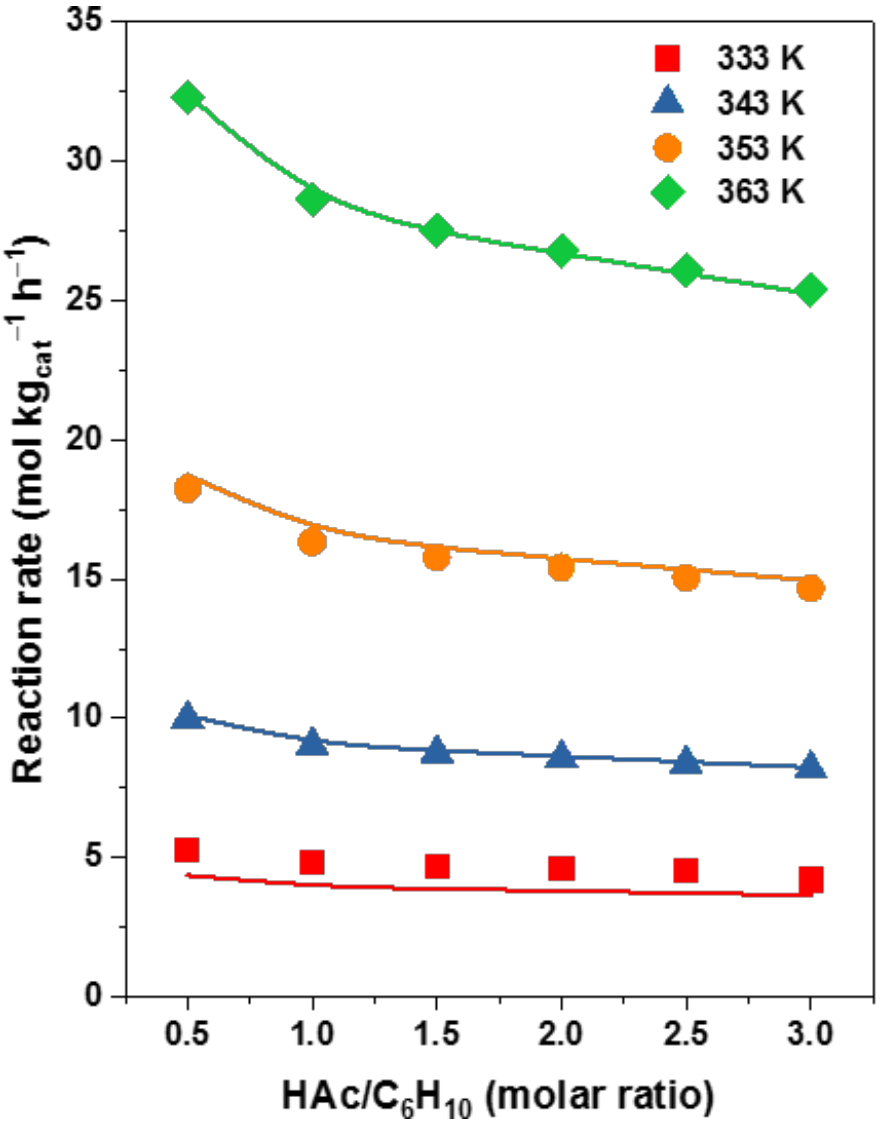

FIGURE 3

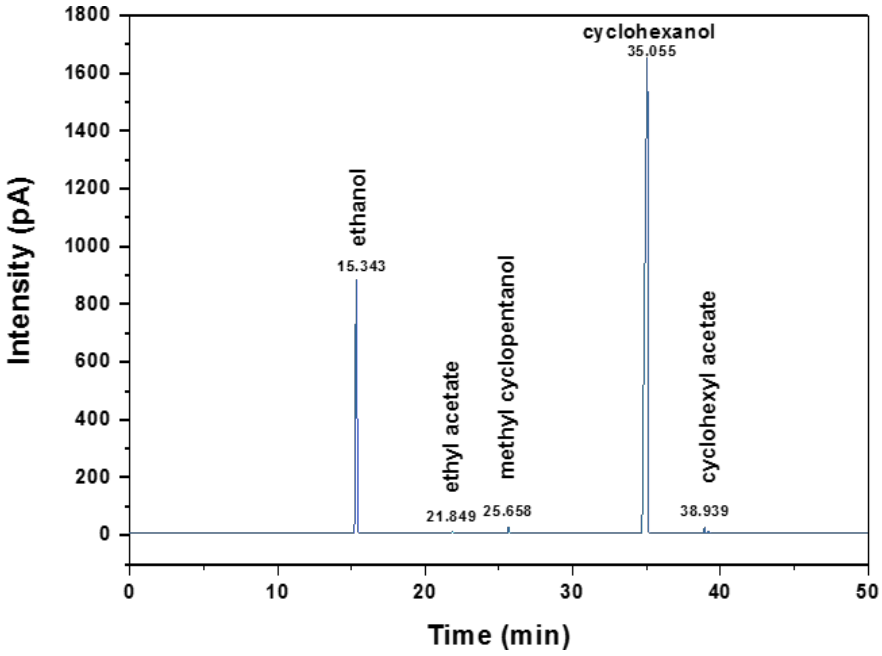

FIGURE 4

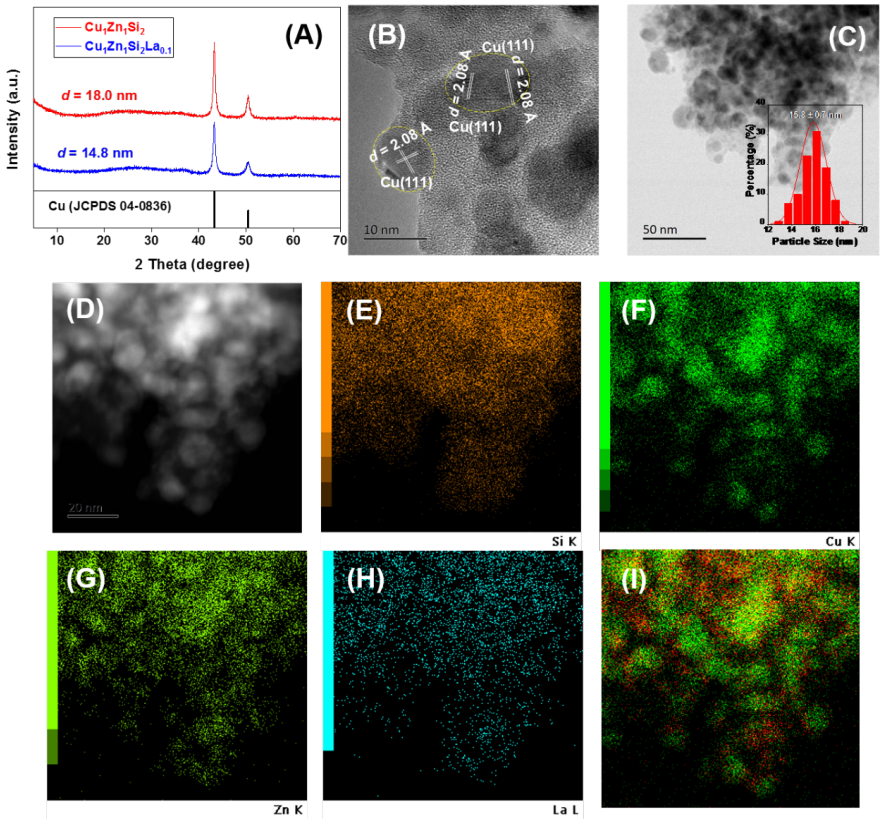

FIGURE 5

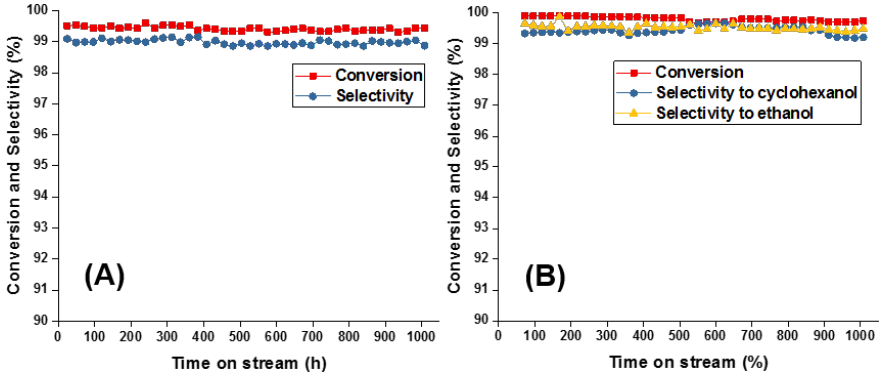

FIGURE 6

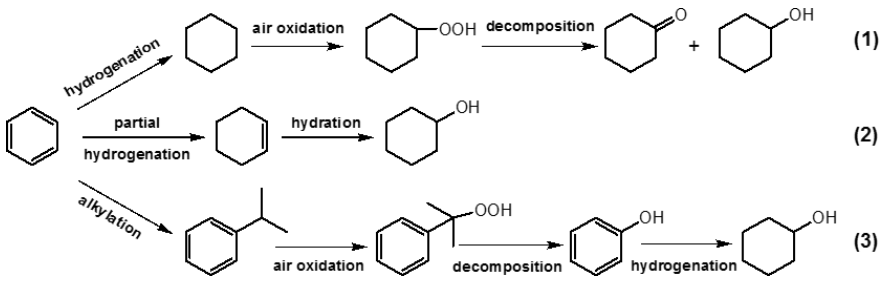

SCHEME 1 Three typical industrialized processes for the production of cyclohexanol/cyclohexanone starting from benzene: (1) cyclohexane oxidation, (2) cyclohexene hydration, and (3) phenol hydrogenation.

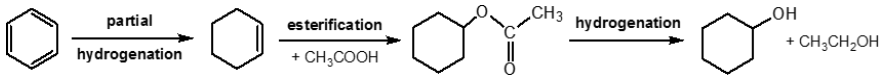

SCHEME 2 The novel cyclohexene esterification–hydrogenation process for the production of cyclohexanol starting from benzene.